ELSEVIER

Modeling nonequilibrium and history effects of homogeneous turbulence in a stably stratified medium

T. P. Sommer,* R. M. C. So,† and J. Zhang‡

*ABB Power Generation Ltd, Gas Turbine and Combined Cycle Development, Baden, Switzerland,
†Mechanical Engineering Department, The Hong Kong Polytechnic University, Hung Hom, Kowloon, Hong Kong, and
‡Mechanical and Aerospace Engineering, Arizona State University, Tempe, AZ

Homogeneous turbulence decay in a stably stratified flow has two distinct characteristics. One is countergradient fluxes that are developed to keep the energy budget in equilibrium. Another is the formation of gravity waves that contribute to the velocity variance with little vertical mixing. The prediction of these characteristics are investigated using a hierarchy of turbulence models. They include second-order models as well as models that solve the transport equations for the turbulent kinetic energy, its dissipation rate, the temperature variance and its dissipation rate. In the latter class of models, the vertical heat flux is calculated either from an algebraic equation or from a transport equation. The algebraic equation is derived by invoking equilibrium and nonequilibrium turbulence assumption. Thus, modeling level and the relative importance of nonequilibrium and history effects in the predictions of countergradient fluxes and gravity waves could be assessed. The investigation reveals that countergradient heat flux can be predicted even when the equilibrium assumption is invoked. However, the formation of gravity waves can be predicted only when the history effects of the vertical heat flux are accounted for properly. The decay rate of the total energy is very much affected by two model constants in the temperature variance dissipation rate equation. On the other hand, the calculated frequency and amplitude of the gravity waves are influenced by the model constants in the heat flux equation.

Keywords: homogeneous turbulence; vertical heat flux; nonequilibrium

Introduction

Stably stratified turbulent flow is a common occurrence in the atmospheric surface layer and in the ocean. Usually the flow is influenced by four different forces; inertia, viscous, buoyancy, and shear forces. Even when there is no mean shear, turbulence in a stably stratified flow still behaves quite differently from that in a nonbuoyant flow. This is because gravity causes anisotropy in the horizontal and vertical velocity variances and their associated length scales. Furthermore, under stable stratification, countergradient fluxes develop to keep the energy budget in equilibrium, and oscillations are formed in the evolution of the Reynolds normal stress aligned with the gravity vector, the temperature variance, and the turbulent vertical heat flux. These oscillations can be interpreted as an exchange of energy between turbulent kinetic energy and potential energy associated with the temperature variance, and these are known as internal gravity waves. The formation of the gravity waves leads to reduced vertical mixing and the ultimate collapse of turbulence (Stillinger et al. 1983; Itsweire et al. 1986; Metais and Herring 1989). Numerous experiments have been carried out to investigate homogeneous turbulence decay in a stably stratified flow. Among the more notable experiments are those of Lienhard and van Atta (1990), Yoon and Warhaft (1990), and Barrett and van Atta (1991). Their measurements clearly indicate the presence of countergradient fluxes but are not as conclusive on the formation of gravity waves. On the other hand, direct numerical simulations (DNS) of such flows have also been carried out by a number of researchers, including the shear flow study of Gerz et al. (1989), the shear and uniform flow investigations of Gerz and Schumann (1991), and the uniform flow study of van Haren et al. (1994). These investigations clearly indicate the development of countergradient fluxes and the formation of gravity waves.

Recent investigations have shown that the initial stages of the evolution of homogeneous turbulence in a stably stratified

Address reprint requests to Dr. R. M. C. So, Department of Mechanical Engineering, The Hong Kong Polytechnic University, Hung Hom, Kowloon, Hong Kong.

Received 10 March 1996; accepted 15 October 1996

Int. J. Heat and Fluid Flow 18: 29–37, 1997

655 Avenue of the Americas, New York, NY 10010

0142-727X/97/$17.00
PII S0142-727X(96)00140-2

medium can be calculated fairly accurately using a k–ε-type model based on an equilibrium assumption (Sommer and So 1995). In the early stages of decay, the agreement between calculations and measurements (Lienhard and van Atta 1990) is comparable to the result of a much more complicated full second-order model (Kolovandin et al. 1993). Particularly, countergradient heat flux is reproduced by the k–ε-type model. In the later stages of the evolution, however, the model of Kolovandin et al., in agreement with experimental data, predicts the formation of gravity waves. Such predictions are absent from the k–ε-type model though.

A number of simplifications have been made in the development of the model of Sommer and So (1995). The most important one is the assumption of equilibrium turbulence, which facilitates the derivation of an algebraic relation for the turbulent heat flux. In reality, the turbulence for the case studied is not in equilibrium. The reason for the discrepancy in the latter stages could, therefore, be attributed to the equilibrium turbulence assumption. If this assumption is the culprit, then a nonequilibrium algebraic relation for the turbulent heat flux could capture the oscillations. On the other hand, history effects in the evolution of the turbulent vertical heat flux might be very important, as indicated by the studies of Kolovandin et al. (1993), van Haren (1993), and Craft et al. (1994).

van Haren (1993) used several one-point closure models to calculate a flow case and compared the results with the DNS data of van Haren et al. (1994). The DNS data, similar to the experimental data of Lienhard and van Atta (1990), exhibits the formation of gravity waves. A simple k–ε model invoking a constant turbulent Prandtl number (Pr_t) fails to replicate any of the important physics, an observation consistent with the findings of Sommer and So (1995). van Haren (1993) proposed an "extended k–ε model" and a "standard second-order model" to calculate the stably stratified flow and found that both models capture the oscillations, and give a reasonably overall agreement with data. However, they predict an oscillation frequency that is lower than that determined from the DNS data. Both these models solve a transport equation each for the turbulent vertical heat flux, the dissipation rate, and the potential energy associated with the temperature variance, while the dissipation of potential energy is calculated assuming a constant time scale ratio. The main difference between the two models is that the "standard second-order model" solves separate equations for the individual Reynolds stresses while the "extended k–ε model" only solves an equation for the turbulent kinetic energy and evaluates the normal velocity variance in the heat flux equation assuming isotropy. Finally, van Haren (1993) used the second-order model of Craft and Launder (1991) and managed to reproduce the correct oscillation frequency. This closure solves a separate equation for the dissipation of potential energy rather than modeling it as in the "standard second-order model." However, it gives a wrong split between kinetic and potential energy.

Use of second-order models to calculate this stably stratified flow has also been attempted by Craft et al. (1994). Their model solves the full set of Reynolds-stress and Reynolds-heat-flux equations, the dissipation rate, and the potential energy equation. The dissipation of the potential energy is modeled rather than determined by solving its transport equation. Buoyancy is accounted for in the following manner. First, the additional explicit term in the dissipation rate (ε) equation is modeled by the proposal of Launder (1989) and setting the additional constant equal to $C_{\varepsilon 1}$, the constant in the modeled destruction term of the nonbuoyant ε-equation. Second, the pressure-strain (Π_{ij}) and pressure-scrambling ($\Phi_{i\theta}$) terms in the Reynolds-stress and Reynolds-heat-flux equations are decomposed into three parts; a slow (return-to-isotropy) part, a rapid (mean strain) part, and a buoyant part, which arises as a result of the buoyancy force acting on the turbulence field. Either simple or fully realizable models can be assumed for the slow, rapid, and buoyant parts of Π_{ij} and $\Phi_{i\theta}$. However, in their model, fully realizable models are invoked for all three parts of Π_{ij} and $\Phi_{i\theta}$. Their investigations show that the model improvements give rise to internal gravity waves whose amplitude and frequency are in good agreement with the DNS data of van Haren et al. (1994).

This discussion shows that there are a number of models with different assumptions that are, to varying degrees, successful in replicating the physics of homogeneous decaying turbulence in a stably stratified medium. It is, however, unclear which features allow certain models to be more successful than the others. Particularly, the following questions are open: Does the failure of the model of Sommer and So (1995) to reproduce the oscillations arise from the equilibrium assumption? Could a nonequilibrium algebraic model capture the gravity waves? Is the better agreement in the oscillation frequency predicted by the model of Craft and Launder (1991) due to the fact that a separate equation for the dissipation of potential energy is solved? Or, is the better agreement due to the solution of turbulence equations where the models assumed are fully realizable?

These questions are difficult to answer because the differences between the various models are too large. This study attempts to provide some answers by using a hierarchy of models based on the same basic transport equations. The baseline model is the second-order model of Lai and So (1990) together with transport equations for the potential energy and its dissipation rate. A hierarchy of models, ranging from the equilibrium algebraic model of Sommer and So (1995), a nonequilibrium model derived in a similar manner and a series of second-order models with different assumptions invoked for the time-scale ratio can be deduced from the basic set of equations. The various models thus derived would allow the different effects, k–ε-type *versus* second-order models, equilibrium *versus* nonequilibrium assumption and history of the heat flux evolution, to be investigated in a systematic manner. In the following, the hierarchy of equations for the second-order and k–ε-type models is presented first. This is followed by a discussion of the model predictions of the stably stratified flow experiment of van Haren et al. (1994). An attempt is made to assess the relative importance of the various assumptions made to derive the models and their impact on the calculations of countergradient fluxes and gravity waves.

Equations for the second-order models

The baseline model equations are the same as those used by Lai and So (1990) to derive their near-wall model. Because of buoyancy, additional equations are necessary for the potential energy and its dissipation rate. There are also some extra model terms in the Reynolds stress and heat-flux equations. Many of the model terms have been suggested by Launder (1976). If the nomenclature of van Haren (1993) is adopted, then the following can be defined. These are the normalized heat flux G, the Brunt–Vaisala frequency N, the potential energy E_{pot}, and the normalized dissipation rate of the potential energy ε_T. They are defined by $G = (g\beta/N)\overline{w\theta}$, $N = [g\beta(d\Theta/dz)]^{1/2}$, $E_{\mathrm{pot}} = (g\beta/N)^2\overline{\theta^2}/2$ and $\varepsilon_T = (g\beta/N)^2\varepsilon_\theta$, where z is the normal coordinate, g is the gravitational constant, β is the coefficient of expansion of the fluid, Θ and θ are the mean and fluctuating temperature, $\overline{w\theta}$ is the normal heat flux, $\overline{\theta^2}$ is the temperature variance, and ε_θ is the dissipation rate of $\overline{\theta^2}$. Thus simplified, the model equations, for the case of homogeneous turbulence in a stratified medium and in the absence of mean shear, can be

written as

$$\frac{d\overline{u^2}}{dt} = -C_1\frac{\varepsilon}{k}\left(\overline{u^2}-\frac{2}{3}k\right)-\frac{2}{3}\varepsilon+C_3\frac{2}{3}NG \quad (1)$$

$$\frac{d\overline{v^2}}{dt} = -C_1\frac{\varepsilon}{k}\left(\overline{v^2}-\frac{2}{3}k\right)-\frac{2}{3}\varepsilon+C_3\frac{2}{3}NG \quad (2)$$

$$\frac{d\overline{w^2}}{dt} = -C_1\frac{\varepsilon}{k}\left(\overline{w^2}-\frac{2}{3}k\right)-\frac{2}{3}\varepsilon+\left(2-2C_3+\frac{2}{3}C_3\right)NG \quad (3)$$

$$\frac{d\varepsilon}{dt} = -C_{\varepsilon 2}\frac{\varepsilon^2}{k}+C_{\varepsilon 3}\frac{\varepsilon}{k}NG \quad (4)$$

$$\frac{dE_{\text{pot}}}{dt} = -NG-\varepsilon_T \quad (5)$$

$$\frac{d\varepsilon_T}{dt} = -C_{d1}\frac{\varepsilon_T}{2E_{\text{pot}}}NG-C_{d2}\frac{\varepsilon}{k}NG-C_{d4}\frac{\varepsilon_T}{2E_{\text{pot}}}\varepsilon_T-C_{d5}\frac{\varepsilon}{k}\varepsilon_T \quad (6)$$

$$\frac{dG}{dt} = -\overline{w^2}N-C_{1\theta}\frac{\varepsilon}{k}G+2N(1-C_{2\theta})E_{\text{pot}} \quad (7)$$

where $k=(\overline{u^2}+\overline{v^2}+\overline{w^2})/2$ is the turbulent kinetic energy, u, v, and w are fluctuating velocities along the x, y, z-coordinates, and ε is the dissipation rate of k. The model constants are the same as those assumed by Sommer and So (1995) and lie within the range suggested by Launder (1976). Their values are: $C_1=1.5$, $C_3=0.3$, $C_{\varepsilon 2}=1.83$, $C_{\varepsilon 3}=1.5$, $C_{1\theta}=3.0$, and $C_{2\theta}=0.4$. As for the constants C_{d1}, C_{d2}, C_{d4}, and C_{d5}, Lai and So (1990) suggested the following values; 1.8, 0, 2.2, and 0.8, respectively. However, it will be seen later that the constants C_{d1} and C_{d2} have a significant influence on the prediction of the total energy decay rate. Their correct values differ from those given above. For easy reference, this model is designated as LS/VTS.

An alternative model can be derived by using a mixed time scale in the heat-flux Equation 7, which then becomes

$$\frac{dG}{dt} = -\overline{w^2}N-C_{1\theta}\sqrt{\frac{\varepsilon}{k}\frac{\varepsilon_T}{2E_{\text{pot}}}}G+2N(1-C_{2\theta})E_{\text{pot}} \quad (8)$$

In this case, the constant $C_{1\theta}$ has to be modified compared to the LS model. If the rationale of So and Sommer (1996) is used to assess its value $C_{1\theta}=3.28$ is obtained. The second-order model comprised of Equations 1–6 and 8 is designated as LS/MTS for easy reference henceforward. It should be pointed out that the only difference between LS/VTS and LS/MTS is in the time-scale assumed in the modeling of the pressure-scrambling vector in the G-equation. The former assumes a velocity time-scale alone; while, the latter invokes a mixed time-scale characteristic of both the velocity and thermal field. Thus, a comparison of the performance of these two models would shed light on the relative importance of mixed *versus* velocity time scale only in the modeling of the transport equation for G.

A third model solves Equations 1–5 and 7, but replaces Equation 6 by a model for the dissipation of potential energy, ε_T. The model for ε_T is given by

$$\varepsilon_T = R\left(\frac{E_{\text{pot}}}{k}\right)\varepsilon \quad (9)$$

where $R=(\varepsilon_T/E_{\text{pot}})/(\varepsilon/k)$ is the time-scale ratio, and its value, taken from van Haren (1993), is $R=1.5$. This model is labeled as LS/FR. A comparison of the performance of LS/FR with LS/VTS could shed light on the relative importance of solving a transport equation for ε_T.

Comparisons are also made with the calculations of the one-point closure model of van Haren (1993) and Craft et al. (1994). The equations solved in the van Haren model are the same as the LS/FR model discussed above. However, the model constants assumed are different, and they are given as: $C_1=1.5$; $C_3=0.5$; $C_{\varepsilon 2}=1.76$; $C_{\varepsilon 3}=1.44$; $C_{1\theta}=4.0$; and $C_{2\theta}=0.33$. This model is designated as VH/FR for easy reference. Thus, a comparison of the performance of LS/FR and VH/FR reveals the effects of the various constants assumed for the modeled equations. On the other hand, the equations solved in the Craft et al. model are similar to those given in Equations 1–7. The exceptions are those models assumed for Π_{ij}, $\Phi_{i\theta}$, and ε_T. Fully realizable models are invoked for Π_{ij} and $\Phi_{i\theta}$. As a result, other heat-flux equations are also solved in addition to Equation 7. Equation 6 is not solved; instead ε_T is modeled assuming the time-scale ratio R in Equation 9 to be replaced by $\tilde{R}$, which is not constant but depends on the heat-flux correlation coefficient. The expression assumed by Craft et al. is $\tilde{R}=3(1+A_{2\theta})/2$, where $A_{2\theta}=\overline{(u_i\theta)(u_i\theta)}/(k\overline{\theta^2})$. This model is designated as CIL/VR for easy reference. In summary, the various models compared are tabulated in Table 1.

Equations for the k–ε-type models

The k–ε model of Sommer and So (1995) consists of solving four transport equations for k, ε, $\overline{\theta^2}$ and ε_θ plus an explicit algebraic equation for the vertical heat flux. Of the four transport equations, the equations for E_{pot} and ε_T are identical to Equations 5 and 6 with the constants as specified in LS/VTS. The equations

Table 1 Summary of the different second-order and k–ε-type models

	Second-order models					k-ε-type models		
	LS/VTS	LS/MTS	LS/FR	VH/FR	CIL/VR	EAHF/E	EAHF/NE	KE/THF
Vel. eqs.	1–4	1–4	1–4	1–4	1–4	10, 11	10, 11	10, 11
Temp. eqs.	5, 6	5, 6	5, 9	5, 9	5, 9 $\tilde{R}$ replaces R in 9	5, 6	5, 6	5, 6
Heat-flux Eqs.	7	8	7	7	7 plus others if required	13	14	7

for k and ε can be written in terms of the present parameters as

$$\frac{dk}{dt} = -\varepsilon + NG \tag{10}$$

$$\frac{d\varepsilon}{dt} = -C_{\varepsilon 2} f_\varepsilon \frac{\varepsilon}{k}\varepsilon + C_{\varepsilon 3}\frac{\varepsilon}{k}NG \tag{11}$$

where the constants assume values given above for LS/VTS and $f_\varepsilon = 1 - 0.22\exp[-(\mathrm{Re}_t/6)^2]$ is a damping function introduced to give a correct prediction of the final decay of k and ε in isotropic turbulence. Here, the turbulence Reynolds number is defined as $\mathrm{Re}_t = k^2/\nu\varepsilon$. The algebraic equation for the heat flux is derived from the simplified transport equation, which can be written as

$$\frac{\overline{u_i\theta}}{k}(\tilde{P} - \varepsilon) + \frac{\overline{u_i\theta}}{\overline{\theta^2}}(2\tilde{P}_\theta - 2\varepsilon_\theta)$$
$$= -\overline{u_i u_j}\frac{\partial\Theta}{\partial x_j} - \overline{u_j\theta}\frac{\partial U_i}{\partial x_j} - C_{1\theta}\sqrt{\frac{\varepsilon}{k}\frac{\varepsilon_\theta}{\overline{\theta^2}}}\,\overline{u_i\theta}$$
$$C_{2\theta}\overline{u_j\theta}\frac{\partial U_i}{\partial x_j} + C_{3\theta}g_i\beta\overline{\theta^2} - g_i\beta\overline{\theta^2} \tag{12}$$

where the transport terms are approximated by invoking the similarity assumption between the transport of heat fluxes and the transport of k and $\overline{\theta^2}$. In Equation 12, $\tilde{P} = -\overline{u_i u_j}(\partial U_i/\partial x_j)$ is the production of k due to mean shear; $\tilde{P}_\theta = -\overline{u_i\theta}(\partial\Theta/\partial x_i)$ is the production of $\overline{\theta^2}$ due to mean temperature gradient; and U_i and x_i are the ith component of the mean velocity and coordinates, respectively. Equilibrium turbulence for both the velocity and thermal fields is assumed by Sommer and So (1995). Consequently, the left-hand side of Equation 12 is identically zero, and the right-hand side can be further simplified by approximating the flux terms associated with the mean gradients by gradient transport models. The result written in terms of the present parameters is

$$G = -C_\lambda k\sqrt{2\frac{k}{\varepsilon}\frac{E_{\mathrm{pot}}}{\varepsilon_T}}\,N + \frac{2(1-C_{2\theta})}{C_{1\theta}}\sqrt{2\frac{k}{\varepsilon}\frac{E_{\mathrm{pot}}}{\varepsilon_T}}\,NE_{\mathrm{pot}} \tag{13}$$

where $C_\lambda = 0.095$ is a model constant assumed for the eddy thermal diffusivity. This model is designated as EAHF/E.

The nonequilibrium algebraic heat-flux model can be derived by following the procedure outlined in Sommer and So (1995), with one exception—that is not to assume the left-hand side of Equation 12 to be zero. Thus derived, the equation for the heat flux can be written as

$$G = \left[-C_\lambda k\sqrt{2\frac{k}{\varepsilon}\frac{E_{\mathrm{pot}}}{\varepsilon_T}}\,N + \frac{2(1-C_{2\theta})}{C_{1\theta}}\sqrt{2\frac{k}{\varepsilon}\frac{E_{\mathrm{pot}}}{\varepsilon_T}}\,NE_{\mathrm{pot}}\right]x$$
$$\left(1 + \frac{2C_\lambda}{C_{1\theta}}\frac{k^2N^2}{\varepsilon\varepsilon_T} - \frac{2}{C_{1\theta}}\sqrt{\frac{k}{2\varepsilon}\frac{\varepsilon_T}{E_{\mathrm{pot}}}} - \frac{1}{C_{1\theta}}\sqrt{\frac{2\varepsilon}{k}\frac{E_{\mathrm{pot}}}{\varepsilon_T}}\right)^{-1} \tag{14}$$

The nonequilibrium model, designated as EAHF/NE, comprises Equations 5, 6, 10, 11, and 14. It differs from EAHF/E in that nonequilibrium effects in the velocity and thermal fields are accounted for in the derivation of the vertical heat flux. However, history effects in the evolution of the normal heat flux are not taken into account. These effects could be accounted for by solving the heat-flux transport Equation 7 together with Equations 5, 6, 10, and 11. To close the set of equations, an additional assumption must be invoked, and this is the isotropic behavior of the velocity field. In other words, $\overline{w^2} = 2k/3$ is assumed in Equation 7. This model is labeled KE/THF. Such a modified k–ε modeling approach has also been investigated by van Haren (1993) and Craft et al. (1994). The present model differs from their models in the choice of the constants assumed and in the modeling of the dissipation rate equations. These models are also listed in Table 1 for easy reference.

Results and discussion

The test case considered here is taken from the numerical experiment of van Haren et al. (1994). The initial flow field consists of homogeneous, isotropic turbulence. At $t = 0$, a constant vertical temperature gradient is applied. The interaction of the turbulence with the temperature gradient leads to the generation of temperature fluctuations; i.e., to increasing potential energy, until the potential energy reaches a maximum. From this point on, oscillations in both potential and kinetic energy occur, with a maximum in kinetic energy coinciding with a minimum in potential energy. The total energy; i.e., the sum of the kinetic and potential energy, decays with a rate slightly smaller than that for the nonbuoyant, isotropic case (van Haren et al. 1994). The initial conditions are given by van Haren (1993) as $k_o = 0.414$, $\varepsilon_o = 0.495$, $\nu = 0.005$, so that $\mathrm{Re}_t = 6925$, and the Brunt–Vaisala frequency is $N = \pi$. The potential energy and its dissipation rate are zero initially. However, to avoid numerical problems, the potential energy is set to a very small value (10^{-9}) at $t = 0$, and ε_T is set assuming $R = 1$. Besides this case, the LS/MTS model is also used to calculate a DNS case where $N = \pi/3$. This case has the same initial conditions as the $N = \pi$ case. Thus, the two cases together will shed light on the effect of Froude number. Numerical tests showed that the results did not exhibit a great sensitivity to the initial values of the potential energy and its dissipation rate, provided they are small enough. The governing modeled equations are solved using a Runge–Kutta method with adaptive step size control (Press et al. 1986) to obtain accurate results with the minimum amount of computational effort. The present objective is to investigate systematically the parameters that contribute to a successful calculation of the development of countergradient fluxes and the formation of gravity waves. Therefore, in addition to evaluating the calculations with the DNS data of van Haren et al. (1994), comparisons with the predictions of van Haren (1993) and Craft et al. (1994) are also carried out. Furthermore, the effects of the model constants, $C_{d1},\ldots,C_{d5}$, and $C_{1\theta}$ and $C_{2\theta}$, on the calculations are examined in detail.

The first set of results is from the k–ε-type models. In this set, the calculations of the models EAHF/E, EAHF/NE, and KE/THF are compared with the DNS data of van Haren et al. (1994) for the case $N = \pi$. The calculations of EAHF/E and EAHF/NE are performed with $C_{d1} = 1.8$ and $C_{d2} = 0$, as specified above. As shown by Sommer and So (1995), these constants would give rise to countergradient heat flux with the EAHF/E model, and the results are in good agreement with the measurements of Lienhard and van Atta (1990). The results of the total ($E_{\mathrm{tot}} = k + E_{\mathrm{pot}}$), kinetic k and potential energy E_{pot} calculated from the EAHF/E, EAHF/NE, and KE/THF models are shown in Figures 1, 2 and 3, respectively. Two sets of results are shown for the KE/THF model in Figure 3; one set is obtained using $C_{d1} = 1.8$ and $C_{d2} = 0$, while another set is given by $C_{d1} = 0$ and $C_{d2} = 1.2$. Vertical heat flux results from the three models and the DNS data are plotted in Figure 4 for comparison. It should

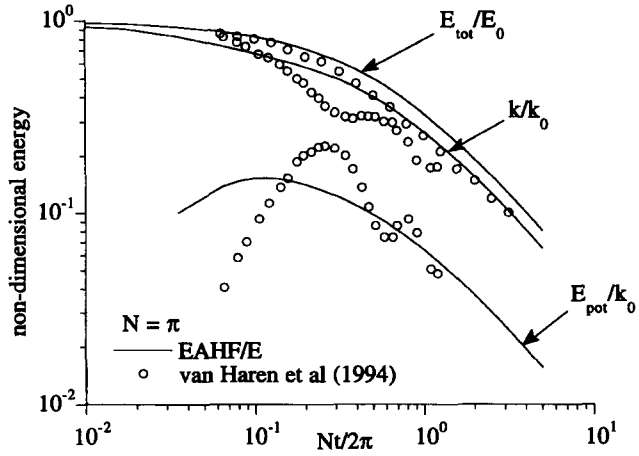

Figure 1 Comparison of the evolution of E_{tot}, k and E_{pot} with DNS data.

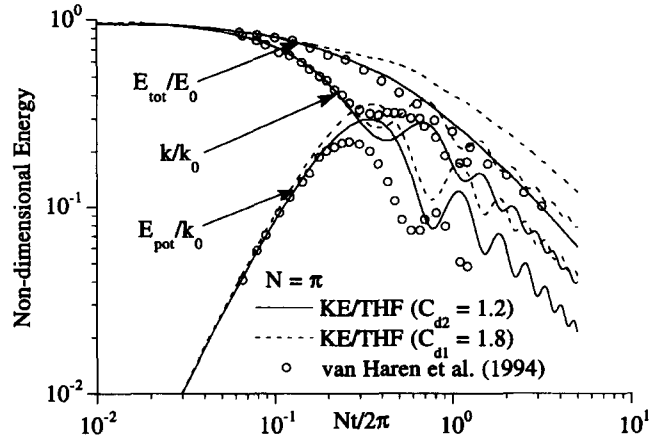

Figure 3 Comparison of the evolution of E_{tot}, k and E_{pot} with DNS data.

be mentioned that, in the course of obtaining the EAHF/NE solutions, a straightforward application of Equation 13 would lead to an unrealistically low E_{pot} result; 3–4 orders of magnitude lower than what it should be. The source of the problem is traced to the similarity assumption used to derive Equation 12. The calculations for this case, therefore, indicate that there might not be any similarity between the transport of heat and the transport of k and $\overline{\theta^2}$. Consequently, the calculations with EAHF/NE are carried out by assuming nonequilibrium of the velocity turbulence field alone, and the results are shown in Figures 2, 4, and 5. This is equivalent to taking the second term on the left-hand side of Equation 12 to be zero. Thus modified, the second and third terms in the second bracketed term of Equation 14 are equal and thus cancelled out each other. In the EAHF/E and EAHF/NE predictions, the growth of E_{pot} is too rapid and its maximum occurs too early (Figures 1 and 2). After reaching the maximum E_{pot}, there are no oscillations, and the decay is too rapid. The absence of oscillations is also apparent in the vertical heat flux, shown for both models in Figure 4. There is a small region of countergradient heat flux which, just as the maximum potential energy, occurs too early. The nonequilibrium assumption, therefore, does not provide visible improvement to the calculation of this case. Thus, both models are unable to predict the $N = \pi$ case correctly.

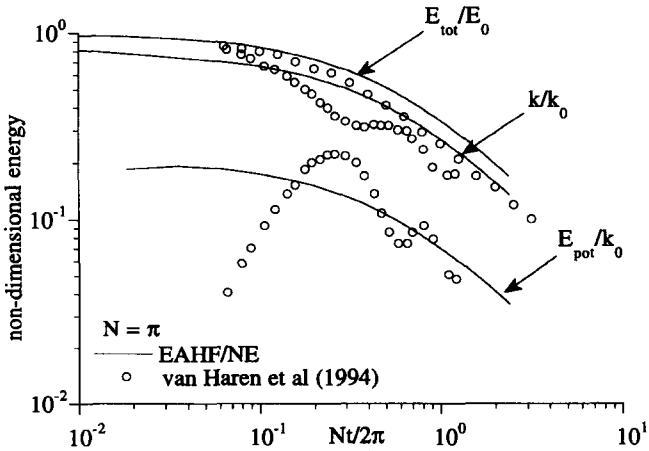

Figure 2 Comparison of the evolution of E_{tot}, k and E_{pot} with DNS data.

Together, these results show the effects of nonequilibrium turbulence and the importance of accounting for the evolution history of the heat flux on the prediction of homogeneous turbulence decay in a stably stratified medium. The formation of gravity waves is predicted only when the heat-flux transport equation is solved. It is found that the constants C_{d4} and C_{d5} do not affect the behavior of the oscillations, but C_{d1} and C_{d2} do. Essentially, varying C_{d1} and C_{d2} change the frequency and period of the predicted oscillations, albeit slightly. However, $C_{d1} = 0$ and $C_{d2} = 1.2$ seem to yield the correct decay rate for E_{tot}/E_o, where E_o is the initial total energy. Therefore, in spite of the incorrect predictions of the frequency and period of the oscillations, overall, the choice of $C_{d1} = 0$ and $C_{d2} = 1.2$ gives better results. On the other hand, if $C_{d1} = 0$ and $C_{d2} = 1.2$ are used in the EAHF/E and EAHF/NE models, the calculated extent of the small region of countergradient heat flux decreases, while the predicted decay rate of E_{tot}/E_o is in much better agreement with the data (Figure 5a). Identical results for this case are also given by any one of the second-order models and KE/THF listed in Table 1. The calculated decay rates of E_{tot}/E_o for the $N = \pi/3$ case using VH/FR, LS/FR, LS/MTS, KE/THF, and EAHF/E models are shown in Figure 5b. Because the model predictions of EAHF/E and EAHF/NE are essentially identical, only the result of EAHF/E is plotted in Figure 5b. In this case, the model calculations are in poor agreement with the DNS data. However, the calculated decay rate of all the models tested does approach the asymptotic

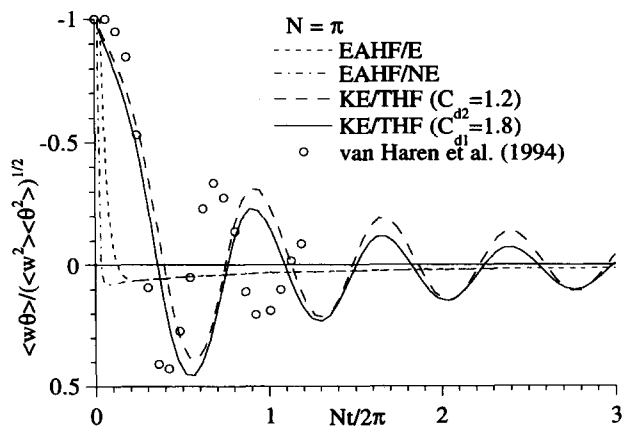

Figure 4 Comparison of the evolution of $\overline{w\theta}$ with DNS data.

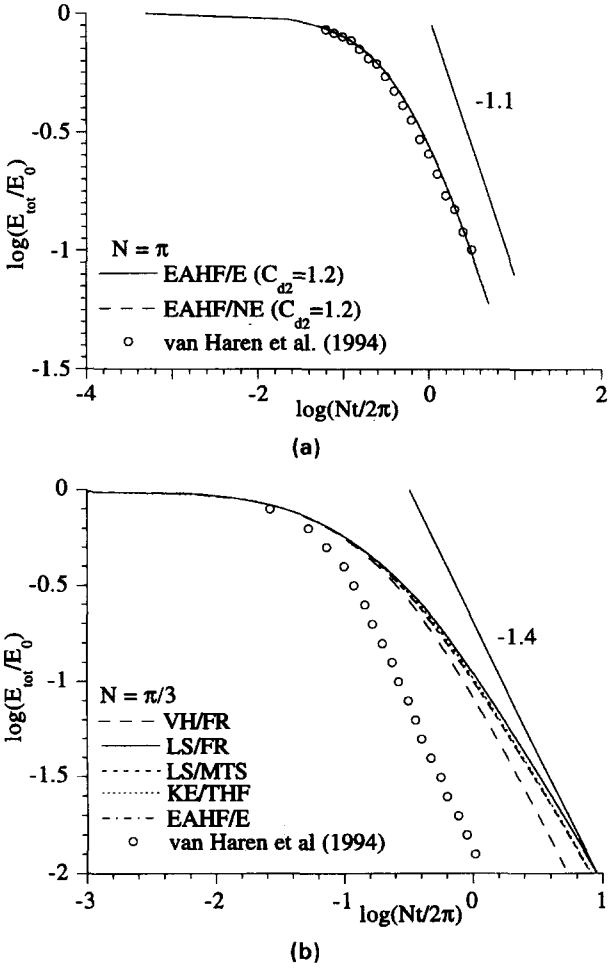

Figure 5 (a) Comparison of the decay rate of E_{tot}/E_0 with DNS data; $N=\pi$ case. (b) Comparison of the decay rate of E_{tot}/E_0 with DNS data; $N=\pi/3$ case.

behavior, a slope of -1.4, correctly at large $Nt/2\pi$. This approach to the slope of -1.4 is not in agreement with the DNS data, however, because the data show a much earlier approach to this asymptotic state. Therefore, it can be said that all the models tested do not perform as well for the $N=\pi/3$ case as for the $N=\pi$ case.

At this point, a comment is in order on the model constants C_{d1} and C_{d2}. In accordance with the findings of the k–ε-type models, the correct decay rates of k and E_{pot} are predicted if, and only if, $C_{d1}=0$ and $C_{d2}=1.2$ are used in the model. Therefore, they are different from those suggested by Sommer and So (1995) for wall turbulence. These new values are consistent with those suggested by Jones and Musonge (1988) and Craft and Launder (1989) for free turbulence. They assumed $C_{d1}=0$ and C_{d2} to be 1.7 and 1.3, respectively. It appears that $C_{d1}=0$ and $C_{d2}\approx 1.2$ are more appropriate for free turbulence.

Having evaluated the relative importance of nonequilibrium and history effects, the next task is to assess the merits, or lack thereof, of second-order modeling. The components of E_{tot}, k, and E_{pot} as calculated using the LS/VTS model are given in Figure 6. It can be seen that the results are in good agreement with DNS data, particularly, the evolution of E_{pot} up to its maximum, and the location of the maximum is well captured. The mean decay of k and E_{pot} are close to the DNS results, as well. There is a slight discrepancy in both the magnitude and the frequency of the oscillations. This can also be observed in the

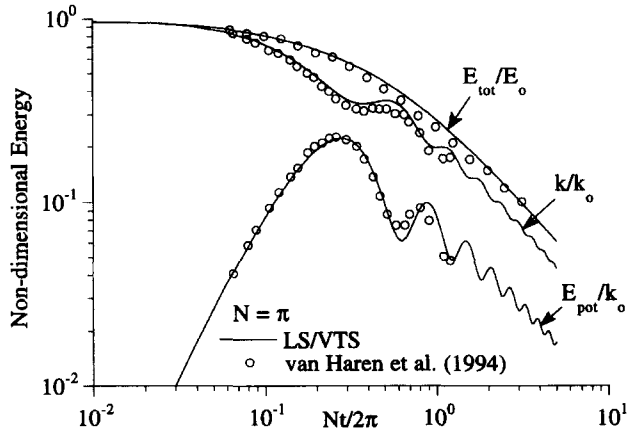

Figure 6 Comparison of the evolution of E_{tot}, k and E_{pot} with DNS data.

calculated heat flux (Figure 7). The frequency of the oscillations is slightly lower compared to that determined from the DNS data.

The importance of solving a transport equation for ε_T is investigated next. This requires the comparison of the calculations obtained from the LS/VTS and LS/FR models. The results are plotted in Figures 8 and 9. Comparing the different plots for the $N=\pi$ case (Figures 6–9), it can be seen that the differences between the various model predictions are, again, not very significant. In fact, the overall agreement of LS/FR predictions with DNS data is about as good as those deduced from LS/VTS and LS/MTS. This comparison shows that the solution of a transport equation for ε_T is not crucial to the prediction of stably stratified flows. An algebraic model for ε_T will suffice.

The relative importance of a velocity *versus* a mixed time-scale in the prediction of the oscillations is examined by comparing the results obtained from LS/VTS and LS/MTS. Results of these calculations are plotted in Figures 10 and 11. Two cases are presented in Figure 11; they are the $N=\pi$ and $N=\pi/3$ case, shown separately in parts (a) and (b) of the figure. The calculated results of the LS/VTS and LS/MTS models are shown together with those of CIL/VR and the DNS data, whenever they are available. These data are extracted from their respective papers. It can be seen that LS/VTS and LS/MTS essentially give the same results. In general, the models perform better for the $N=\pi$ case than for the $N=\pi/3$ case (see Figure 5b for decay rate). Furthermore, the amplitude of the oscillations obtained

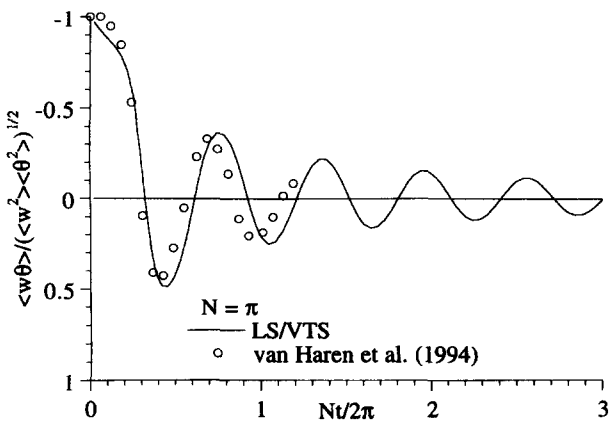

Figure 7 Comparison of the evolution of $\overline{w\theta}$ with DNS data.

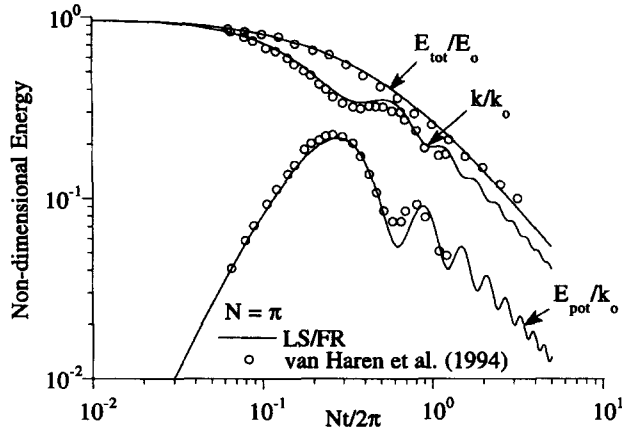

Figure 8 Comparison of the evolution of E_{tot}, k and E_{pot} with DNS data.

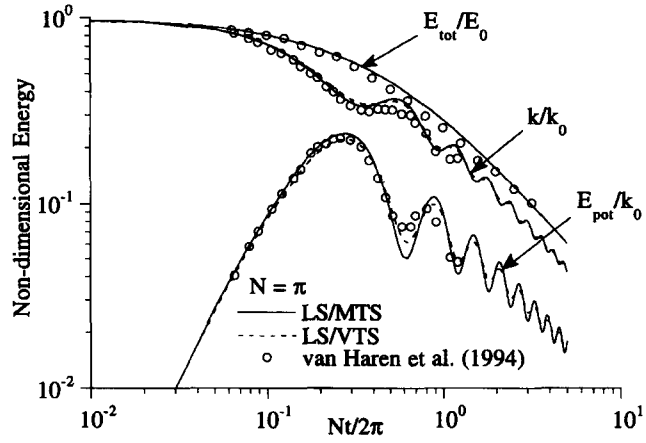

Figure 10 Comparison of the evolution of E_{tot}, k and E_{pot} with DNS data; $N=\pi$ case.

from the LS/MTS model is larger than that deduced from the LS/VTS model, however, the frequency is about the same (Figures 10 and 11). This comparison shows that the time-scale invoked in the modeling of the pressure-scrambling term in the heat-flux equation has little or no effect on the prediction of stably stratified turbulent flows. On the other hand, relaxing the isotropic assumption in the heat-flux equation has a very significant effect on the prediction of the oscillations, their amplitude and frequency (compared Figures 3, 6, and 10). This means that a second-order model is critical to the successful prediction of stably stratified turbulent flows.

The effect of Π_{ij} and $\Phi_{i\theta}$ modeling on the prediction of the oscillations can be studied by comparing the calculations of LS/MTS with those of CIL/VR. These two closures not only differ in the models assumed for Π_{ij} and $\Phi_{i\theta}$, but also in the modeling of ε_T. While LS/MTS solves Equation 6, CIL/VR invokes an algebraic model for ε_T. Because the effect of modeling ε_T is not important in the prediction of the oscillations, the variations noted in the LS/MTS and CIL/VR results could then be attributed to the different Π_{ij} and $\Phi_{i\theta}$ models invoked. The result for one case is compared in Figure 11. Overall, CIL/VR gives a slightly more accurate predictions of the amplitude and frequency of the oscillations. Therefore, the fully realizable Π_{ij} and $\Phi_{i\theta}$ models used in CIL/VR do provide an advantage over the much simpler Π_{ij} and $\Phi_{i\theta}$ models adopted by Lai and So (1990).

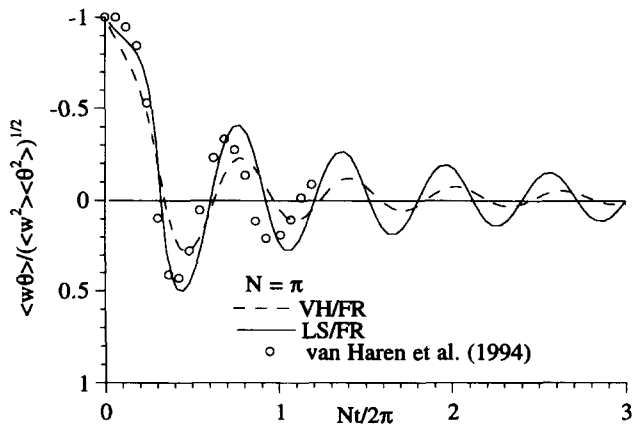

Figure 9 Comparison of the evolution of $\overline{w\theta}$ with DNS data.

Finally, the influence of the model constants $C_{1\theta}$ and $C_{2\theta}$ on the prediction of the oscillations is examined. The first comparison is carried out with two different models, VH/FR and LS/FR, which assume $C_{1\theta}=4.0$ and $C_{1\theta}=3.0$, respectively. The results for the $N=\pi$ case are shown in Figures 9 and 12. It can be seen that the VH/FR model yields an oscillation amplitude and

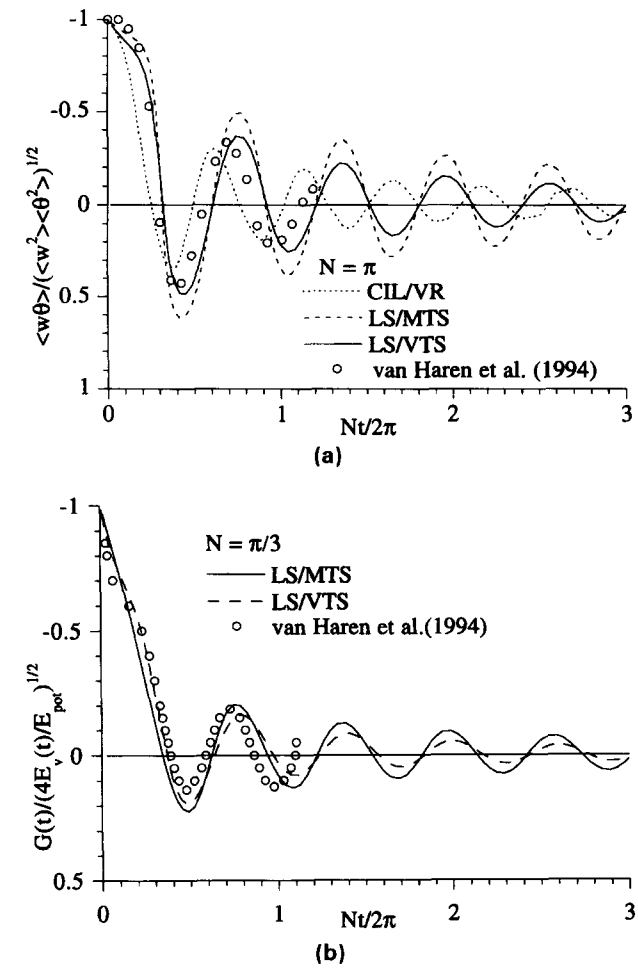

Figure 11 (a) Comparison of the evolution of $\overline{w\theta}$ with DNS data; $N=\theta$ case. (b) Comparison of the evolution of $\overline{w\theta}$ with DNS data: $N=\pi/3$ case.

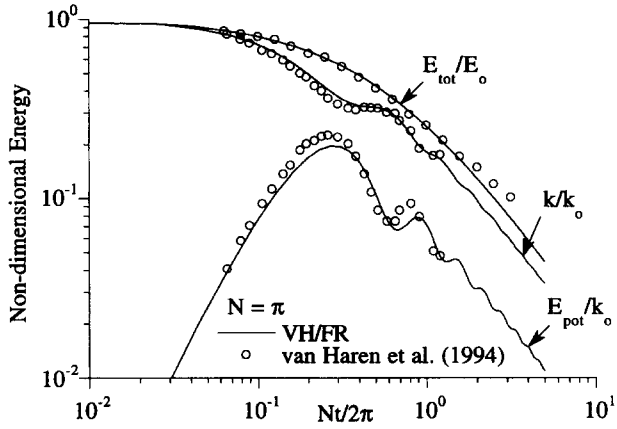

Figure 12 Comparison of the evolution of E_{tot}, k and E_{pot} with DNS data.

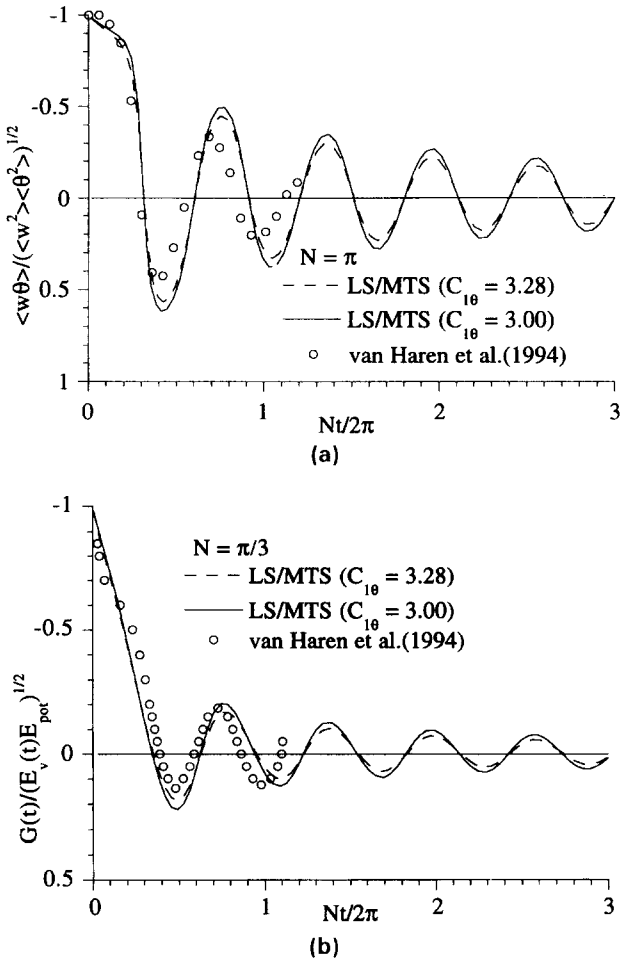

Figure 13 (a) Comparison of the evolution of $\overline{w\theta}$ with DNS data for two different values of $C_{2\theta}$. (b) Comparison of the evolution of $\overline{w\theta}$ with DNS data for two different values of $C_{2\theta}$.

frequency quite different from those deduced from the DNS data. Furthermore, the calculated amplitude and frequency of the oscillations are also different from those determined from LS/FR, which are in better agreement with the data (see Figures 8 and 9). It appears that a decrease of $C_{1\theta}$ by 25% is sufficient to obtain an oscillation frequency and amplitude that agree about as closely with the data as the results van Haren (1993) obtained using the model of Craft and Launder (1991). The effect of varying $C_{1\theta}$ using the same model, LS/MTS, is shown in Figures 13a and 13b. The values of $C_{1\theta}$ are chosen as 3.28 and 3.00, while all other model constants are kept the same as before. It can be seen that, for both cases, decreasing $C_{1\theta}$ reduces the amplitude of the oscillations slightly, and there is a very small effect on the calculated frequency. These effects seem to be independent of N. On the other hand, the effect of $C_{2\theta}$ on the calculation of the oscillations is examined in Figures 14a and 14b. In this calculation, $C_{1\theta} = 3.00$ is chosen, and all other model constants in LS/MTS remain unchanged, except $C_{2\theta}$, which takes on a value of 0.4 and 0.1, respectively. The results show that decreasing $C_{2\theta}$ improves the predicted frequency of the oscillations but not the amplitude. Again, the effects seem to be independent of N. However, there is really no justification to assume $C_{2\theta} = 0.1$.

Conclusions

Three k–ε-type models and three second-order models derived from the same set of basic equations are used to assess the relative importance of the following simplifications in the prediction of homogeneous turbulence decay in a stably stratified medium. They are the equilibrium, nonequilibrium, and isotropic assumptions and the evolution history of the vertical heat flux. Furthermore, the study also examines the necessity of solving a transport equation for ε_T and the effects of the model constants invoked in this equation and the vertical heat-flux equation on the calculations. The EAHF/E and EAHF/NE models fail to reproduce the essential physics of the turbulence. Particularly, they are unable to reproduce the oscillations associated with the exchange of energy between turbulent kinetic and potential energy. Thus, it is not sufficient to account for nonequilibrium effects alone in the calculation of stably stratified flows. All models solving a transport equation for the heat flux, on the other hand, predict the formation of gravity waves or the existence of the oscillations. However, the assumption of turbulence isotropy renders the predictions of the oscillation frequency and amplitude incorrect, as can be seen from the results of KE/THF compared with LS/VTS. It can, therefore, be concluded that gravity waves can only be predicted correctly if history effects are taken into account, and turbulence isotropy is not assumed. The results show further that it is not essential in this case to solve a separate equation for ε_T; it is sufficient to model its behavior algebraically. Furthermore, the present investigation reveals that the model constants C_{d1} and C_{d2} affect the calculated total energy decay, while the constant $C_{1\theta}$ has a greater effect on the predicted oscillation amplitude than on its frequency. On the other hand, the constant $C_{2\theta}$ affects the calculated frequency but not the amplitude. If $C_{2\theta} = 0.1$ is chosen, the calculated frequency is in good agreement with the $N = \pi$ case. However, there is no justification to decrease $C_{2\theta}$ substantially to 0.1. In view of these findings, it can be concluded that the model LS/FR with $R = 1.5$ and $C_{1\theta} = 3.0$ performs just as well as the model LS/VTS. Finally, comparisons are also made with the model results of Craft et al. (1994). Their closure differs in the modeling of the pressure-strain tensor and pressure-scrambling vector, which are given by fully realizable models, and in the treatment of the dissipation rate of the potential energy. Although their predictions are in better agreement with DNS data in terms of both the amplitude and frequency of the oscillations, the slight improvements do not justify the adoption of much more complicated pressure–strain and pressure-scrambling models.

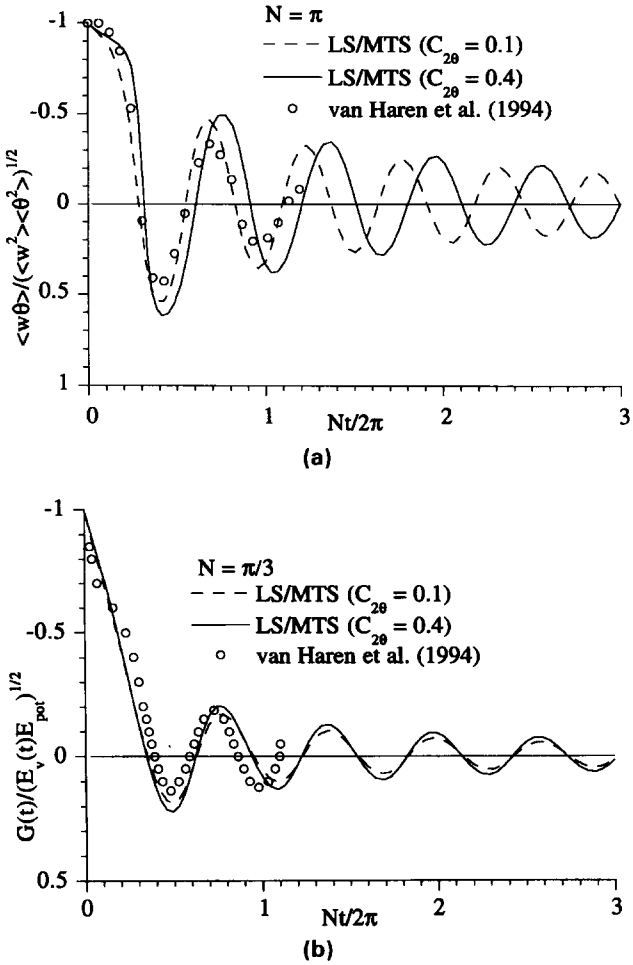

Figure 14 (a) Comparison of the evolution of $\overline{w\theta}$ with DNS data for two different values of $C_{1\theta}$. (b) Comparison of the evolution of $\overline{w\theta}$ with DNS for two different values of $C_{1\theta}$.

Acknowledgments

Funding support for RMCS during his tenure at the Mechanical and Aerospace Engineering Department, Arizona State University, Tempe, AZ, and JZ under Grant PL0008587-AG, Knolls Atomic Power Laboratory, Schenectady, NY is gratefully acknowledged. The grant was monitored by R. Kunz.

References

Barrett, T. K. and van Atta, C. W. 1991. Experiments on the inhibition of mixing in stably stratified decaying turbulence using laser-Doppler-anemometry and laser-induced fluorescence. *Phys. Fluids A*, **3**, 1321–1332

Craft, T. J. and Launder, B. E. 1989. A new model for the pressure/scalar-gradient correlation and its application to homogeneous and ingomogeneous free shear flows. *Proc. 7th Symposium on Turbulent Shear Flows*, (Paper no. 12-4), Stanford, CA

Craft, T. J. and Launder, B. E. 1991. Computation of impinging flows using second-moment closures. *Proc. 8th Symposium on Turbulent Shear Flows*, September 7–9 (Paper 8-5), Munich, Germany

Craft, T. J., Ince, N. Z. and Launder, B. E. 1994. Recent developments in second-moment closure for buoyancy-affected flows, *Proc. 4th Int. Symposium on Stratified Flow*, LEGI/Institut Mecanique de Grenoble, June 29–July 2, Vol. 2

Gerz, T. and Schumann, U. 1991. Direct simulation of homogeneous turbulence and gravity waves in sheared and unsheared stratified flows, In *Turbulent Shear Flows 7*, F. Durst et al, (eds.), Berlin, Germany, 27–46

Gerz, T., Schumann, U. and Elghobashi, S. 1989. Direct numerical simulation of stratified homogeneous turbulent shear flow. *J. Fluid Mech.*, **200**, 563–594

Itsweire, E. C., Helland, K. N. and van Atta, C. W. 1986. The evolution of grid-generated turbulence in a stably stratified fluid. *J. Fluid Mech.*, **162**, 299–338

Jones, W. P. and Musonge, P. 1988. Closure of the Reynolds-stress and scalar flux equations. *Phys. Fluids*, **31**, 3589–3604

Kolovandin, B. A., Bondarchuk, V. U., Meola, C. and De Felice, G. 1993. Modeling of the homogeneous turbulence dynamics of stably stratified media. *Int. J. Heat Mass Transfer*, **36**, 1953–1968

Lai, Y. G. and So, R. M. C. 1990. Near-wall modeling of turbulent heat fluxes. *Int. J. Heat Mass Transfer*, **33**, 1429–1440

Launder, B. E. 1976. Heat and Mass Transport. In *Topics in Physics*, P. Bradshaw (ed.), Springer, New York, 231–287

Launder, B. E. 1989 The Prediction of Force-Field Effects on Turbulent Shear Flow via Second-Moment Closure. In *Advances in Turbulence-2*, H. H. Fernholz and H. E. Fiedler (eds.), Springer-Verlag, Berlin, 338–358

Lienhard, J. H. and van Atta, C. W. 1990. The decay of turbulence in thermally stratified flow. *J. Fluid Mech.*, **210**, 57–112

Metais, O, and Herring, J. R. 1989. Numerical simulation of freely evolving turbulence in stably stratified fluids. *J. Fluid Mech.*, **202**, 117–148

Press, W. H., Flannery, B. P., Teukolsky, S. A. and Vetterlink, W. T. 1986. *Numerical Recipes—The Art of Scientific Computing*, Cambridge University Press, Cambridge, UK, 563–568

So, R. M. C. and Sommer, T. P. 1996. An explicit algebraic heat-flux model for the temperature field. *Int. J. Heat Mass Transfer*, **39**, 455–465

Sommer, T. P. and So, R. M. C. 1995. On the modeling of homogeneous turbulence in a stably stratified flow, *Phys. Fluids*, **7**, 2766–2777

Stillinger, D. C., Helland, K. N. and van Atta, C. W. 1983. Experiments on the transition of homogeneous turbulence to internal waves in a stratified fluid. *J. Fluid Mech.*, **131**, 91–122

van Haren, L., Staquet, C., and Cambon, C. 1994. A study of decaying stratified turbulence by a two-point closure EDQNM model and by direct numerical simulations. *Proc. 4th Int. Symposium on Stratified Flows*, Grenoble, France, June 29–July 2

van Haren, L. 1993. Etude theorique et modelisation de la turbulence en presence d'ondes internes. These de doctorat, Ecole Centrale de Lyon, 141–156

Yoon, K. and Warhaft, Z. 1990. The evolution of grid-generated turbulence under conditions of stable thermal stratification. *J. Fluid Mech.*, **215**, 601–638